



Materials Science in Semiconductor Processing 10 (2007) 159-166

MATERIALS SCIENCE IN **SEMICONDUCTOR PROCESSING**

Absolute band gap engineering of anisotropic square and triangular photonic crystals

B. Rezaei^{a,b,*}, M. Kalafi^{a,b}

^aResearch Institute for Applied Physics and Astronomy, Tabriz University, P.O. Box 51665-163, Tabriz, Iran ^bExcellence Center for Photonics, University of Tabriz, Tabriz, Iran

Available online 7 November 2007

Abstract

We analyze the band gap properties of two-dimensional photonic crystals created by square and triangular lattices of rods, considering that the rods are formed of a dielectric core surrounded by an interfacial layer of anisotropic tellurium. Using the plane wave analysis, we study the modification of the band gap spectrum when the rods are infiltrated with different dielectric core and discuss the optimization strategies leading to the maximum value of the absolute band gap. © 2007 Elsevier Ltd. All rights reserved.

PACS: 42.70.Qs; 78.20.Ci; 78.20.Bh

Keywords: Photonic band gap; Anisotropic tellurium rods; Dielectric core

1. Introduction

In recent years, photonic band gap (PBG) materials, called photonic crystals, have attracted great interest as it can be an efficient control of the electromagnetic (EM) radiation and can affect the properties of photons in much the same way as semiconductors affect the properties of electrons [1,2]. One of the major features of the photonic crystals is their ability to prevent the propagation of light in some frequency regions due to the existence of absolute PBGs in the transmission spectrum.

Unlike the most potential applications of the three-dimensional photonic crystals, two-dimen-

*Corresponding author. Tel.: +984113393027; fax: +984113347050.

E-mail addresses: b rezaei@tabrizu.ac.ir,

rezaeibhr@yahoo.com (B. Rezaei).

sional ones are easier to fabricate, especially for the technologically important near-infrared or visible spectrum. Much attention has, therefore, been paid to two-dimensional photonic crystals. Since the PBG is the major feature of a PBG structure, it is essential to design a structure that possesses a forbidden gap as large as possible. So many attempts, such as symmetry reduction [3] and anisotropy in dielectricity [4], have been made to enlarge the PBG in two-dimensional photonic crystals.

To our knowledge, only a few investigations have been made to demonstrate how the existence of an interfacial (or cladding) layer affects the values and properties of photonic gaps [5-7]. In fact, such interfacial layers can appear around holes in macroporous silicon after etching and they can strongly influence the properties of band gap spectrum [6]. In addition, it has been reported that the use of tellurium hollow rods [7] may have a dramatic effect on the absolute band gap due to the properties of the photonic crystals fabricated from anisotropic materials.

More recently, the interest in the study of the properties of complex photonic crystals with interfacial layers has been enhanced by the effort to model the void-based photonic crystals created by a femtosecond laser-driven micro-explosion method where a change in the refractive index in the region surrounding the void dots that form the bcc structures is verified experimentally [8]. In addition, the recently suggested class of the so-called annular photonic crystals [9], where dielectric rods are embedded into air holes of larger radius, fit the same category of complex structures where the air space can be regarded as an additional interfacial layer.

In this paper, we analyze the band gap spectra of two-dimensional anisotropic photonic crystals created by square and triangular lattices of hollow anisotropic tellurium rods and study the properties of the absolute PBG when the hollow rods are filled by another material.

2. Lattice description and numerical method

To determine absolute PBGs in periodic dielectric structures, we study the propagation of light from Maxwell's equations. In inhomogeneous dielectric materials, the Maxwell's equation for the magnetic field yields [10–13]

$$\nabla \times \left[\frac{1}{\varepsilon(\vec{r})} \nabla \times H(\vec{r}) \right] = \frac{\omega^2}{c^2} H(\vec{r}), \tag{1}$$

where ω is the frequency of light and c is the light velocity. The dielectric constant $\varepsilon(\vec{r})$ is a periodic function of \vec{r} in x-y plane and satisfies the condition $\varepsilon(\vec{r}+\vec{R})=\varepsilon(\vec{r}), \ \vec{R}$ denotes real space lattice vectors. Since $\varepsilon(\vec{r})$ is periodic, we can use Bloch's theorem to expand the $H(\vec{r})$ as the sum of plane waves:

$$H(\vec{r}) = \sum_{\vec{G}} \sum_{\lambda=1}^{2} h_{\vec{G},\lambda} \hat{e}_{\lambda} e^{i(\vec{K} + \vec{G}) \cdot \vec{r}}, \qquad (2)$$

where \vec{k} is a wave vector in the first Brillouin zone and \vec{G} is a two-dimensional reciprocal lattice vector, $\hat{e}_{\lambda}(\lambda=1,2)$ are orthogonal unit vectors perpendicular to $\vec{k} + \vec{G}$. So, Eq. (1) is expressed as a linear matrix equation for the dispersion of

EM waves:

$$\sum_{\vec{G}'} H_{\vec{G},\vec{G}'} \binom{h_{\vec{G}',1}}{h_{\vec{G}',2}} = \frac{\omega^2}{c^2} \binom{h_{\vec{G},1}}{h_{\vec{G},2}}, \tag{3}$$

where

$$H_{\vec{G},\vec{G}'} = |\vec{k} + \vec{G}||\vec{k} + \vec{G}'|\eta(\vec{G} - \vec{G}') \begin{bmatrix} \hat{e}_2 \cdot \hat{e}'_2 & -\hat{e}_2 \cdot \hat{e}'_1 \\ -\hat{e}_1 \cdot \hat{e}'_2 & \hat{e}_1 \cdot \hat{e}'_1 \end{bmatrix},$$
(4)

where $\eta(\vec{G})$ is the Fourier transform of the inverse of $\varepsilon(\vec{r})$, and it plays a key role in determination of photonic band structure. We study a periodic array of dielectric rods with the property that their extension direction is parallel to the z-axis and the intersection of these rods with the x-y plane forms a two-dimensional periodic dielectric structure. In this case, the Fourier coefficients are given by

$$\eta(\vec{G}) = \frac{1}{\Omega} \int_{\text{cell}} \varepsilon^{-1}(\vec{r}) e^{-i\vec{G}\cdot\vec{r}} \, d\vec{r}. \tag{5}$$

Here we designate the surface of unit cell by Ω . In a two-dimensional photonic crystal $\vec{k} + \vec{G}$ is in the x-y plane for all \vec{G} so we can choose all \hat{e}_1 and \hat{e}_2 vectors parallel to the z direction and in the x-y plane, respectively. In this case, $\hat{e}_2 \cdot \hat{e}_1' = \hat{e}_1 \cdot \hat{e}_2' = 0$.

For light incident perpendicular to the rod axis, the matrix Eq. (4) decouple into two scalar problems, corresponding to two polarizations. In the case of *E*-polarization ($E(\vec{r})$ is parallel to the rod axis), $h_{\vec{G},1} = 0$ for all \vec{G} and we have

$$\sum_{\vec{G}'} |\vec{k} + \vec{G}| |\vec{k} + \vec{G}'| \eta(\vec{G} - \vec{G}') h_{\vec{G}',2} = \frac{\omega^2}{c^2} h_{\vec{G},2}.$$
 (6)

For the *H*-polarization ($H(\vec{r})$ is in the rod axis), $h_{\vec{G},2} = 0$ for all \vec{G} and the eigenvalue equation becomes

$$\sum_{\vec{G}'} (\vec{k} + \vec{G}) \cdot (\vec{k} + \vec{G}') \eta (\vec{G} - \vec{G}') h_{\vec{G}', 1} = \frac{\omega^2}{c^2} h_{\vec{G}, 1}.$$
 (7)

The structures under consideration and the corresponding first Brillouin zones are shown in Fig. 1. We have considered (a) square and (b) triangular structures of circular shape rods with dielectric constant $\varepsilon_{\rm r}$ of inner rod and anisotropic outer shell, embedded periodically in a background of dielectric constant $\varepsilon_{\rm b}$. The anisotropic outer shell layer has two different principle refractive indices as ordinary-refractive index $n_{\rm o}$ and extraordinary refractive index $n_{\rm e}$.

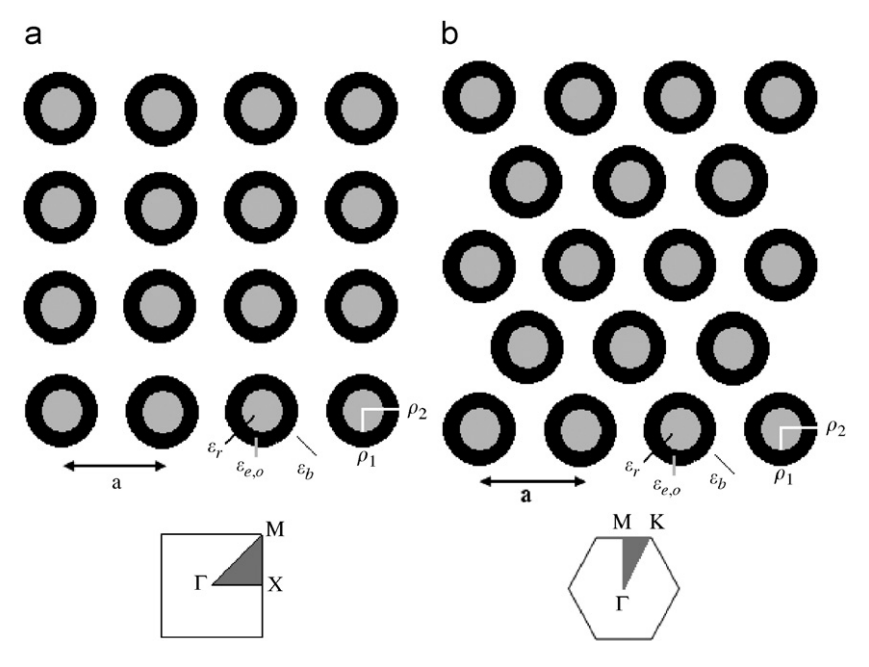


Fig. 1. Schematic diagrams of studied structures: (a) square and (b) triangular lattices of rods covered by anisotropic tellurium interfacial layer and the corresponding first Brillouin zones.

We assume that the extraordinary axis is parallel to the z-axis. In this configuration, the eigen equations for the E- and H-polarization modes are the same as those for the isotropic photonic crystals, except that the dielectric indices of anisotropic outer shell are $n_{\rm e}$ and $n_{\rm o}$ for E- and H-polarizations, respectively. The corresponding dielectric constant is expressed as

$$\frac{1}{\varepsilon(\vec{r})} = \frac{1}{\varepsilon_{b}} + (\frac{1}{\varepsilon_{r}} - \frac{1}{\varepsilon_{b}}) \sum_{\vec{R}} P_{\text{rod}}(\vec{r} - \vec{R})
+ \left(\frac{1}{\varepsilon_{e,o}} - \frac{1}{\varepsilon_{b}}\right) \sum_{\vec{R}} P_{\text{shell}}(\vec{r} - \vec{R}),$$
(8)

where $\varepsilon_{\rm e}=n_{\rm e}^2$ and $\varepsilon_{\rm o}=n_{\rm o}^2$, $P_{\rm rod}$ and $P_{\rm shell}$ describe the probability of finding the inner rod and shell, respectively and can be expressed as

$$P_{\text{rod}}(\vec{r}) = \begin{cases} 1, & \vec{r} \in R_{\text{rod}}, \\ 0, & \vec{r} \notin R_{\text{rod}}, \end{cases}$$

$$P_{\text{shell}}(\vec{r}) = \begin{cases} 1, & \vec{r} \in R_{\text{shell}}, \\ 0, & \vec{r} \notin R_{\text{shell}}. \end{cases}$$

$$(9)$$

where $R_{\rm rod}$ and $R_{\rm shell}$ are the regions in the x-y plane defined by the cross section of the inner rod and outer shell, respectively. The Fourier coefficients of $\varepsilon^{-1}(\vec{r})$ according to Eq. (5) can be

written as

$$\eta(\vec{G}) = \begin{cases} \frac{1}{\varepsilon_{b}} + \frac{\pi\rho_{1}^{2}}{\Omega} \left(\frac{1}{\varepsilon_{r}} - \frac{1}{\varepsilon_{b}}\right) + \frac{\pi}{\Omega} (\rho_{2}^{2} - \rho_{1}^{2}) \left(\frac{1}{\varepsilon_{e,o}} - \frac{1}{\varepsilon_{b}}\right), & \vec{G} = 0, \\ \frac{2\pi}{\Omega G} \left\{ \left(\frac{1}{\varepsilon_{r}} - \frac{1}{\varepsilon_{b}}\right) \rho_{1} J_{1}(\rho_{1} G) + \left(\frac{1}{\varepsilon_{e,o}} - \frac{1}{\varepsilon_{b}}\right) [\rho_{2} J_{1}(\rho_{2} G) - \rho_{1} J_{1}(\rho_{1} G)] \right\}, & \vec{G} \neq 0, \end{cases}$$

$$(10)$$

where $J_1(x)$ is the Bessel function of the first kind. ρ_1 and ρ_2 are the radius of the inner rod and the outer radius of the shell layer, respectively.

3. Results and discussion

For this study, two-dimensional square and triangular photonic crystal of circular rods consisting of an inner rod with dielectric constant ε_{r} and anisotropic outer shell aligned in a uniform background with dielectric constant ε_{b} has been considered.

The band structure of two-dimensional photonic crystal is obtained numerically by solving Eqs. (6) and (7). A total of 441 plane waves were used for both structures in these calculations, which ensures sufficient convergence for the frequencies of interest. Our main goal here is to study the modification of the band gap spectrum and the value of the absolute

band gap when the thickness of outer shell (interfacial layer) varies, as well as when the rods are infiltrated with other materials (dielectric core).

We have chosen tellurium (Te) as the anisotropic interfacial layer, which has a positive uniaxial crystal with principle indices of $n_{\rm e}=6.2$ and $n_{\rm o}=4.8$. The dielectric constant of background is $\varepsilon_{\rm b}=1$. In these structures three geometrical parameters ρ_1 , ρ_2 , and $\varepsilon_{\rm r}$ are treated as adjustable parameters to obtain the maximum absolute PBG.

We begin our discussion with the square structure (Fig. 1(a)). First, we consider the case when there is

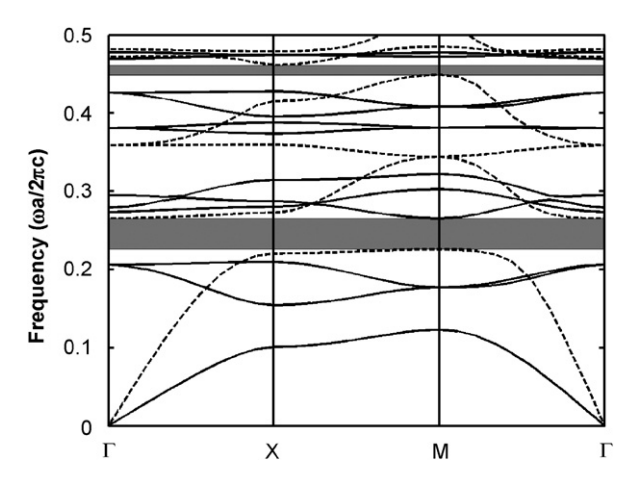


Fig. 2. Photonic band spectrum of square lattice of tellurium rods in air background for E-(solid) and H-(dashed) polarization modes at optimum value of $\rho_2 = 0.36a$.

no core dielectric constant (solid tellurium rods), i.e. $\rho_1 = 0$. Fig. 2 shows the photonic band structure for optimum value of $\rho_2 = 0.36a$, the lattice constant being a. This frequency spectrum displays two absolute PBGs and a relatively large one at lower frequency. The large absolute band gap lies between 0.2256 and 0.2648 frequencies in units of $2\pi c/a$ with maximum normalized width $\Delta\omega = 0.0392(2\pi c/a)$.

At next step, the inner spaces of rods are filled with other materials. In this case, for a given value of ε_r , the inner rod radius ρ_1 is optimized to obtain the maximum absolute PBG at fixed optimum value of $\rho_2 = 0.36a$. So, we study how the filling of tellurium rods with different dielectric constants may change the size and position of the maximum absolute PBG. Fig. 3 shows the variation of absolute PBG size at optimum value of $\rho_2 = 0.36a$ when the inner rod radius, ρ_1 , ranges from 0 to 0.27a and the dielectric core, $\varepsilon_{\rm r}$, ranges from 1 to 22. We can see from Fig. 3 that absolute PBG reaches its maximum value at optimum inner rod radius $\rho_1 = 0.22a$ when the dielectric core is $\varepsilon_r = 16.5$. The photonic band structure of this case is shown in Fig. 4. It can be seen that the large absolute PBG size is $\Delta \omega = 0.0434(2\pi c/a)$ and lies between 0.2356 and 0.279 frequency regions in units of $2\pi c/a$.

For a comprehensive investigation, we have also done such calculations for different tellurium radius (ρ_2) . After extensive calculations, we have found that the optimal parameters for the largest absolute

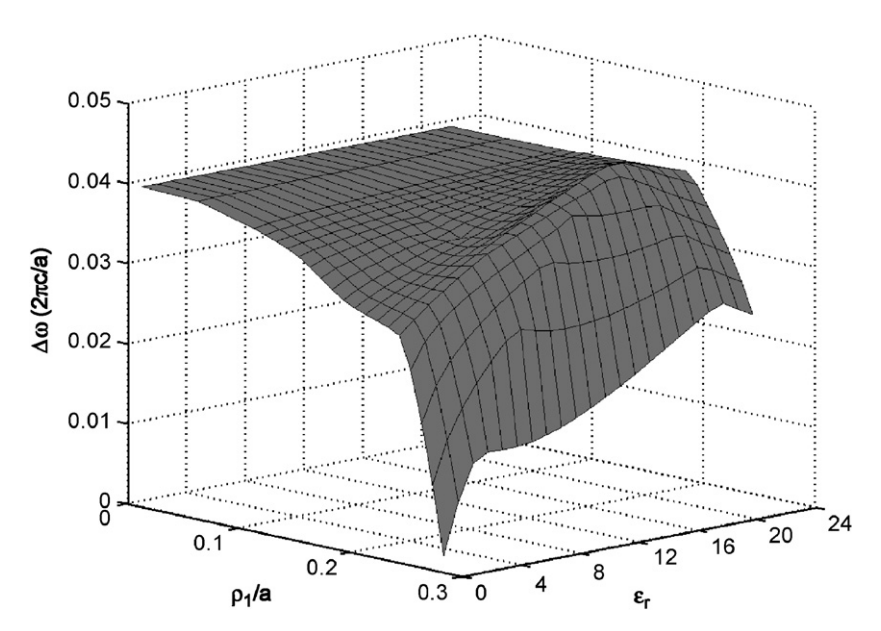


Fig. 3. Variation of absolute band gap size at optimum value of external radius $\rho_2 = 0.36a$ for square lattice when the internal radius and the dielectric core range from 0 to 0.27a and from 1 to 22, respectively.

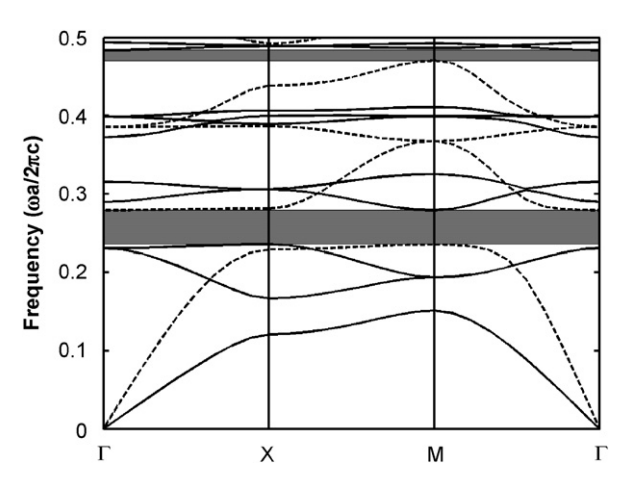


Fig. 4. Photonic band spectrum of square lattice of rods with anisotropic tellurium interfacial layer for *E*-(solid) and *H*-(dashed) polarization modes. The optimum values of parameters are $\varepsilon_r = 16.5$, $\rho_1 = 0.22a$ and $\rho_2 = 0.36a$.

PBG are $\rho_1=0.18a$, $\rho_2=0.3a$, and $\varepsilon_r=1$ (i.e. the hollow Te rods). The photonic band structure for these geometrical parameters is displayed in Fig. 5, for which the absolute PBG reaches its maximum normalized width of $\Delta\omega=0.0481(2\pi c/a)$ and lies between 0.3149 and 0.363 frequencies in units of $2\pi c/a$.

Also, the band structure of hollow isotropic dielectric rods with an average refractive index of $n_{\rm av} = (n_{\rm e} + 2n_{\rm o})/3 = 5.26$ for both polarization modes at the same optimal parameters, i.e. $\rho_1 =$ 0.18a, $\rho_2 = 0.3a$, and $\varepsilon_r = 1$ is shown in Fig. 6. This frequency spectrum shows several band gaps for the E-polarization mode (solid) and a band gap for H-polarization mode (dashed), but they do not overlap with each other to create an absolute PBG. However, the case can be changed by choosing different refractive index constants for the E- and H-polarization modes. This will enable the optimal overlapping of band gaps to obtain an absolute PBG. Since anisotropic materials have two kinds of different dielectric constants for the E- and H-polarization modes, we can obtain the largest absolute PBG by matching the relative positions of band gaps for the two polarization modes [4]. This can be clearly seen from Fig. 5, which shows that because of the properties of anisotropic material, the H 1–2 band gap (i.e. the gap between the first and second photonic bands) moves upwards and overlaps with the E 3-4 band gap, thus a complete PBG is opened. Our results show that the gap behavior is governed by the dielectric core and anisotropy in dielectricity. By optimizing the inter-

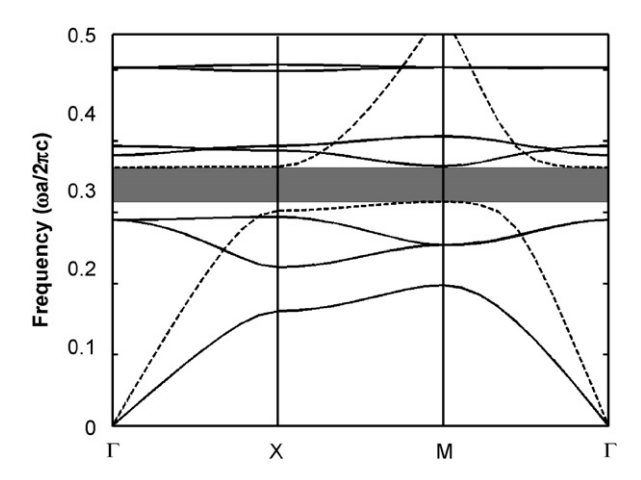


Fig. 5. Photonic band spectrum of square lattice of rods with anisotropic tellurium interfacial layer for *E*-(solid) and *H*-(dashed) polarization modes at optimal parameters $\varepsilon_{\rm r}=1$, $\rho_1=0.18a$ and $\rho_2=0.3a$.

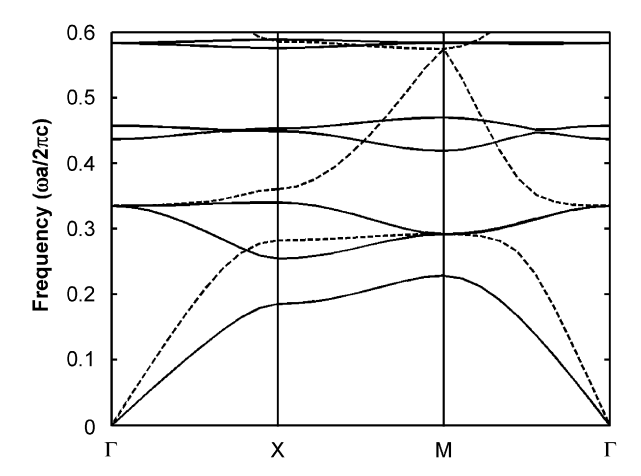


Fig. 6. Photonic band spectrum of square lattice of rods with isotropic interfacial layer for *E*-(solid) and *H*-(dashed) polarization modes. The refractive index for isotropic layer is $n_{\rm av} = 5.26$ and optimal parameters are $\varepsilon_{\rm r} = 1$, $\rho_1 = 0.18a$ and $\rho_2 = 0.3a$.

nal rod and dielectric core for several values of tellurium radius, we have found a large absolute PBG for two-dimensional square lattice of rods covered by anisotropic cladding layer. Obviously, compared with the case of solid tellurium rods, the size of the large absolute PBG has been increased and shifted to higher frequencies a little.

Tellurium is a kind of positive uniaxial crystal with unusually large principle indices $n_{\rm e}=6.2$ and $n_{\rm o}=4.8$ in the infrared wavelength regime. Although it is a semiconductor material, its free carrier absorption is quite weak in the infrared regime. Taking into account the fabrication limits, the large absolute PBG for this structure is centered

at $\omega a/2\pi c=0.3389$ for $\rho_1=0.18a$ and $\rho_2=0.3a$. In the infrared wavelength range, it is possible to center the PBG at $\lambda=1.6\,\mu\mathrm{m}$, which is an important wavelength in optical communication, by realizing the square lattice of hollow tellurium rods of $\rho_1=0.1\,\mu\mathrm{m}$ and $\rho_2=0.16\,\mu\mathrm{m}$ separated by a distance $a=0.54\,\mu\mathrm{m}$.

Now, we concentrate on the triangular lattice consisting of rods covered with anisotropic tell-urium interfacial layer (Fig. 1(b)). In the case of solid tellurium rods ($\rho_1 = 0$), the dispersion relation for triangular structure of tellurium rods in air

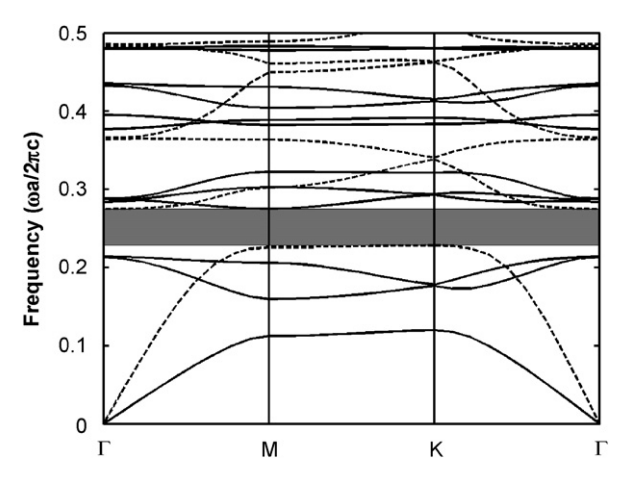


Fig. 7. Photonic band spectrum of triangular lattice of tellurium rods in air background for *E*-(solid) and *H*-(dashed) polarization modes at optimum value of $\rho_2 = 0.355a$.

background ($\varepsilon_b = 1$) has been shown in Fig. 7 for optimum value of $\rho_2 = 0.355a$. This frequency spectrum displays an absolute PBG with maximum normalized width of $\Delta\omega = 0.047(2\pi c/a)$ and lies between 0.2279 and 0.2749 frequencies in units of $2\pi c/a$.

Next, similar to the pervious case, we study the evolution of absolute PBG at optimum value of external radius ($\rho_2 = 0.355a$) when the tellurium rods are infiltrated with another material. Fig. 8 displays the variation of absolute band gap size when the internal radius, ρ_1 , ranges from 0 to 0.27a and the dielectric core, ε_r , ranges from 1 to 22. It can be seen that the absolute PBG size has the largest value $\Delta \omega = 0.0542(2\pi c/a)$ at optimum internal radius $\rho_1 = 0.2a$ when the dielectric core $\varepsilon_r = 13$. Fig. 9 plots the dispersion relation for this case. We can see that the absolute PBG lies between 0.239 and 0.2932 frequencies in units of $2\pi c/a$. The same calculations have been done for other values of tellurium radius. Extensive investigations show that the maximum absolute PBG is obtained for triangular lattice with optimal geometrical parameters $\rho_1 = 0.2a$, $\rho_2 = 0.3a$, and $\varepsilon_r = 2$. In Fig. 10 we plot the dispersion relation for this case, which shows an absolute PBG with maximum normalized width $\Delta \omega = 0.0668(2\pi c/a)$ between 0.3286 and 0.3954 frequencies in units of $2\pi c/a$. Compared to the case of solid tellurium rods the size of absolute PBG has been increased and its position has been

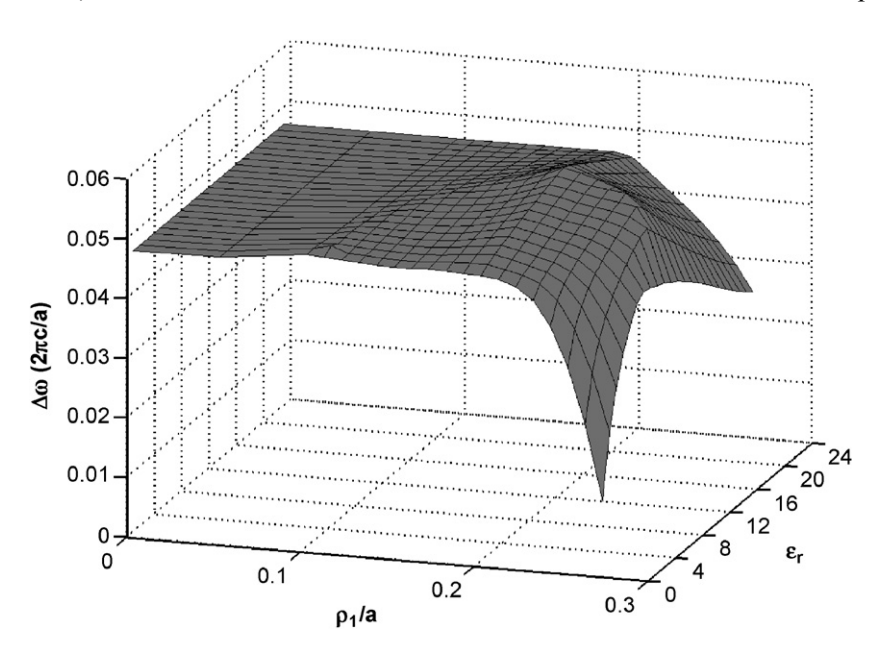


Fig. 8. Variation of absolute band gap size at optimum value of external radius $\rho_2 = 0.355a$ for triangular lattice when the internal radius and the dielectric core range from 0 to 0.27a and from 1 to 22, respectively.

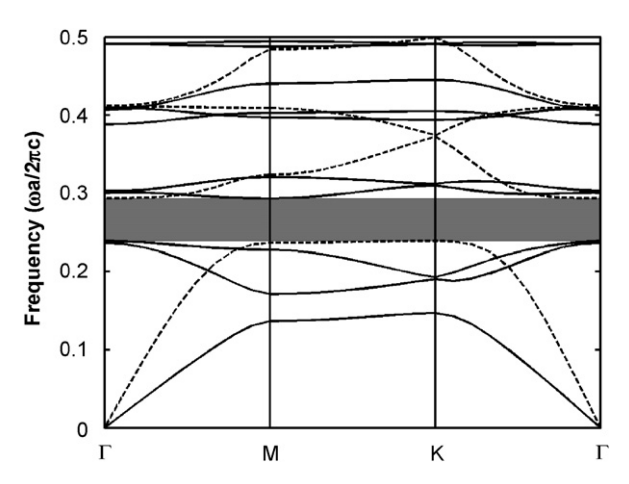


Fig. 9. Photonic band spectrum of triangular lattice of rods with anisotropic tellurium interfacial layer for *E*-(solid) and *H*-(dashed) polarization modes. The optimum values of parameters are $\varepsilon_r = 13$, $\rho_1 = 0.2a$ and $\rho_2 = 0.355a$.

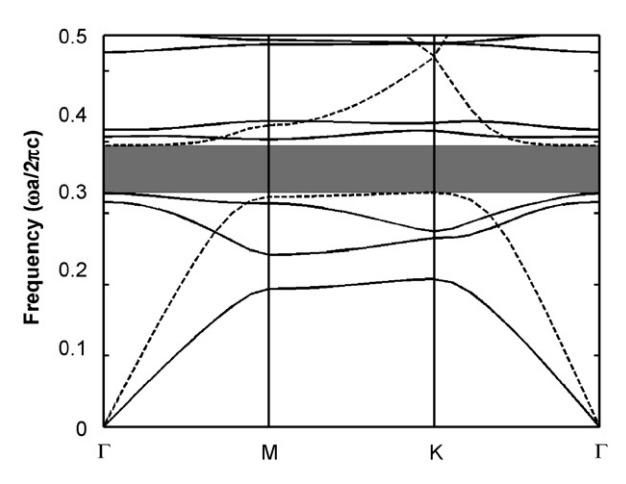


Fig. 10. Photonic band spectrum of triangular lattice of rods with anisotropic tellurium interfacial layer for *E*-(solid) and *H*-(dashed) polarization modes at optimal parameters $\varepsilon_r = 2$, $\rho_1 = 0.2a$ and $\rho_2 = 0.3a$.

shifted to higher frequencies. The mid-gap frequency is $\omega a/2\pi c=0.362$ and can be matched to $\lambda=1.6\,\mu\mathrm{m}$ when $a=0.58\,\mu\mathrm{m}$, $\rho_1=0.12\,\mu\mathrm{m}$, and $\rho_2=0.17\,\mu\mathrm{m}$.

In Fig. 11 we also plot the dispersion relation for triangular lattice of isotropic material with an average refractive index $n_{\rm av} = 5.26$ at optimal parameters $\rho_1 = 0.2a$, $\rho_2 = 0.3a$, and $\varepsilon_{\rm r} = 2$. From this figure one sees that a complete band gap does not exist in this case. Similar to the square lattice, an optimal absolute band gap can be obtained by matching the relative position of the H 1–2 band gap with the E 3–4 band gap by introducing the anisotropy in the dielectric of shell layer (Fig. 10).

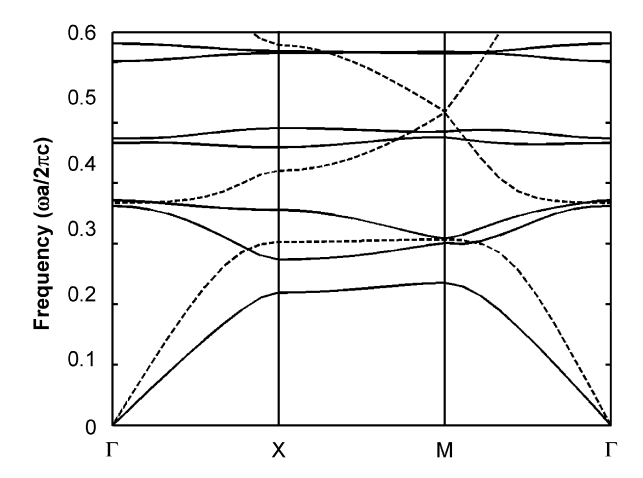


Fig. 11. Photonic band spectrum of triangular lattice of rods with isotropic interfacial layer for *E*-(solid) and *H*-(dashed) polarization modes. The refractive index for isotropic layer is $n_{\rm av} = 5.26$ and optimal parameters are $\varepsilon_{\rm r} = 2$, $\rho_1 = 0.2a$ and $\rho_2 = 0.3a$.

The main result is that for triangular lattice of rods surrounded by anisotropic shell layer, the value and properties of absolute PBG are strongly affected by core dielectric constants and properties of anisotropic materials. The greatest absolute PBG has been obtained for this structure by optimizing the inner and external rod radius for different values of dielectric core.

4. Conclusion

We analyze the band gap properties of twodimensional photonic crystals created by square and triangular lattices of rods, considering that the rods are formed of a dielectric core surrounded by an interfacial layer of anisotropic tellurium. Using the plane wave analysis, we have studied different aspects of the modification of the band gap spectrum when the rods are infiltrated with different dielectric core. We have discussed and demonstrated several optimization strategies leading to the maximum value of the absolute band gap in such anisotropic photonic crystals.

Acknowledgments

The authors are indebted to Yuri Kivshar (Canberra, Australia) for useful discussions and suggestions. This work was supported by the Excellence Center for Photonics of the University of Tabriz, Iran.

References

- [1] Yablonovitch E. Phys Rev Lett 1987;58:2059.
- [2] John S. Phys Rev Lett 1987;58:2486.
- [3] Trifonov T, Marsal LF, Rodriguez A, Pallares J, Alcubilla R. Phys Rev B 2004;69:235112.
- [4] Li ZY, Gu BY, Yang GZ. Phys Rev Lett 1998;81:2574.
- [5] Pan T, Li Z-Y. Solid State Commun 2003;128:187.
- [6] Trifonov T, Marsal LF, Rodriguez A, Pallares J, Alcubilla R. Phys Rev B 2004;70:195108.
- [7] Pan T, Zhuang F, Li Z-Y. Solid State Commun 2004; 129:501.

- [8] Zhou G, Ventura MJ, Gu M, Mattews AF, Kivshar YuS. Opt Express 2005;13:4390.
- [9] Kurt H, Citrin DS. Opt Express 2005;13:10316.
- [10] Joannopoulos JD, Meade RD, Winn JN. Photonic crystals: molding the flow of light. Princeton: Princeton University Press; 1995.
- [11] Plihal M, Maradudin AA. Phys Rev B 1991;44:8565.
- [12] Ho KM, Chan CT, Soukoulis CM. Phys Rev Lett 1990; 65:3152
- [13] Busch K, John S. Phys Rev E 1998;58:3896.